Amplified warming of extreme temperatures over tropical land

Michael P. Byrne[1,2]

November 15, 2022

[1]*School of Earth & Environmental Sciences, University of St Andrews, UK*
[2]*Department of Physics, University of Oxford, UK*

Abstract

Extreme temperatures have warmed substantially over recent decades and are projected to continue warming in response to future climate change. Warming of extreme temperatures is amplified over land, with severe implications for human health, wildfire risk and food production. Using simulations from 18 climate models, I show that hot days over tropical land warm substantially more than the average day. For example, warming of the hottest 5% of land days is a factor of 1.21 ± 0.07 larger than the time-mean warming averaged across models. The climate-change response of extreme temperatures over tropical land is interpreted using a theory based on atmospheric dynamics. According to the theory, warming is amplified for hot land days because those days are dry: this is termed the "drier get hotter" mechanism. Changes in near-surface relative humidity further increase tropical land warming, with decreases in land relative humidity particularly important. The theory advances physical understanding of the tropical climate and highlights land-surface dryness as a key factor determining how extreme temperatures respond to climate change.

Warming of extreme temperatures has large human[1] and economic impacts[2] particularly over land where the warming is strongest[3]. The land-ocean warming contrast – whereby annual-mean near-surface temperatures increase more rapidly over land relative to ocean[4, 5, 6, 7, 8, 9] – implies strong warming of extreme land temperatures even in the absence of changes in temperature variability[10]. But increases in temperature variability with climate change further amplify warming of extreme land temperatures[11], with soil moisture feedbacks playing a key role in mid-latitude regions[11, 12, 13, 14, 15, 16, 10]. Temperature advection[17, 18, 19], atmospheric circulation anomalies[20] and local thermodynamics[21] also shape mid-latitude temperature extremes – both cold and hot – and their response to climate change.

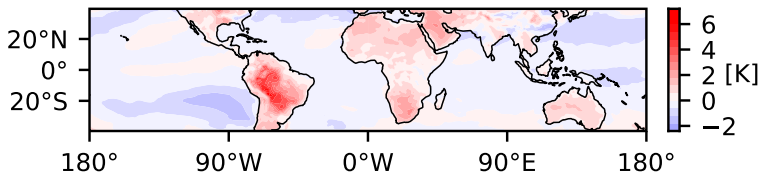

Figure 1: **Projected warming of the hottest 5% of days relative to the zonal-mean warming.** Surface-air temperature change averaged over the hottest 5% of days at each gridpoint between the *historical* (1980-2000) and Shared Socioeconomic Pathway 4.5 [*ssp245*] (2080-2100) simulations for the GFDL-CM4 model. To highlight the differing responses of extreme temperatures over land and ocean, anomalies with respect to the zonal-mean change at each latitude are shown.

Compared to the rapidly advancing knowledge of extreme temperatures in mid-latitudes[15, 18, 22, 23, 20, 19, 21], understanding of extremes over tropical land remains limited. Extreme temperatures in the tropics are only weakly influenced by temperature advection[24] and atmospheric blocking – often the driver of extreme events in mid-latitudes[25] – does not typically occur at low latitudes[26]. Soil moisture feedbacks partially account for the amplified warming of extreme temperatures over tropical land[14]. But the effects of soil moisture on surface temperature are complex[27], vary considerably across climate models[10] and are challenging to quantify *a priori* (i.e. without running a climate model). The limited understanding of extreme temperatures over tropical land – compounded by incomplete long-term temperature records[28] – compares unfavourably with the burgeoning understanding of mid-latitude extreme temperatures and robust theories for precipitation and snow extremes in a changing climate[29, 30, 31]. With tropical regions emerging as a hotspot of intensifying heatwaves[32, 33], a quantitative theory for extreme temperatures over tropical land is needed to interpret and underpin projections from climate models and address a notable gap in our understanding of the Earth system.

Amplified warming of hot days

Here I show, using simulations with climate models together with a theory based on atmospheric dynamics, that the response to climate change of extreme temperatures over tropical land – defined here as high percentiles of daily-mean near-surface temperature – can be explained by ocean warming and humidity over land and ocean. In particular, amplified warming of hot land days is driven by those days being dry; I term this the "drier get hotter" mechanism. Simulations from 18 climate models contributing to the World Climate Research Programme's Coupled Model Intercomparison Project Phase 6[34] are analysed (Methods). Climate change is defined as the difference between the *historical*

and Shared Socioeconomic Pathway[35] 4.5 (*ssp245*) simulations. Land between 20°S and 20°N is analysed as the assumptions supporting the theory are primarily applicable to tropical regions[8, 9, 36].

Projected warming of extreme temperatures is amplified over tropical land (Fig. 1). Averaged across models, daily-mean near-surface tropical temperatures exceeding the 95th percentile warm by 3.5 K ± 0.9 K over land compared to 2.0 K ± 0.5 K over ocean (Fig. 2a). Note that all uncertainties quoted in the text are standard deviations across models. Warming of high percentiles of land temperature is strongly amplified relative to the mean warming[37] (Fig. 2b), implying a change in the shape of the temperature distribution. The higher the percentile the greater the amplification, with the hottest 5% of land days warming by a factor of 1.21 ± 0.07 more than the mean day. Consistent with previous work[38], amplified warming of extreme temperatures is weak over tropical oceans where the hottest 5% of days warm by only a factor of 1.02 ± 0.04 more than the mean day (Fig. 2b).

A theory for extreme temperatures over tropical land

I now introduce a theory to understand the response of extreme temperatures over tropical land to climate change. In the tropics, active atmospheric convection[39] couples near-surface moist static energy to free-tropospheric temperature. Moist static energy h is conserved under moist adiabatic processes and, near the surface, is a function of temperature and specific humidity:

$$h = c_p T + L_v q, \tag{1}$$

where T and q are the near-surface temperature and specific humidity, respectively, c_p is the specific heat capacity of air at constant pressure and L_v is the latent heat of vapourisation. Temperatures in the tropical free troposphere are approximately uniform in the horizontal because the effect of Earth's rotation is weak at low latitudes; this is known as the Weak Temperature Gradient (WTG) approximation[40]. The vertical coupling of moist static energy to free-tropospheric temperature by convection, combined with the WTG approximation, constrains changes in near-surface moist static energy to be roughly uniform across the tropics and, therefore, equal over land and ocean[41, 42, 9, 36, 43]. Individually, temperature and specific humidity over land and ocean respond very differently to climate change[4, 5, 6, 7, 8, 44, 41, 45, 9]. But their combined response (specifically the moist static energy change) is approximately uniform across the tropics because of dynamical processes – convection and weak rotation – connecting the atmospheres above land and ocean regions[9].

I use this dynamical constraint to develop a theory for the response of extreme temperatures over tropical land to climate change (see Methods for the full derivation). The key assumption is that changes in moist static energy percentiles are equal over land and ocean:

$$\delta h_{\mathrm{L}}(p) = \delta h_{\mathrm{O}}(p), \tag{2}$$

where $h(p)$ is the p-th percentile of near-surface moist static energy over land (L) or ocean (O) and δ denotes a change between the historical and ssp245 simulations. Compared to changes in percentiles of temperature or specific humidity, which show clear land-ocean contrasts, changes in moist static energy percentiles are roughly equal over land and ocean, particularly for high percentiles (Fig. 3). Ocean relative humidity is approximately constant under climate change[46, 47], meaning that changes in near-surface ocean specific humidity are primarily controlled by changes in sea-surface temperature. Constant ocean relative humidity therefore implies – together with (2) – that ocean warming alone constrains changes in high percentiles of moist static energy over land.

The coupling between moist static energies over land and ocean is the basis of the theory for extreme temperatures over tropical land. To transform (2) into an equation for the land temperature response, I first assume that the change in land moist static energy averaged over all days exceeding the x-th percentile of temperature – defined as $\delta h_{\mathrm{L}}^{x}$ – is equal to the change in ocean moist static energy (δh_{O}) plus a contribution (Δh) to account for hot land days becoming relatively less energetic under climate change:

$$\delta h_{\mathrm{L}}^{x} = \delta h_{\mathrm{O}}(p^{x}) + \Delta h, \tag{3}$$

where p^{x} is defined as the moist static energy percentile over land corresponding to the average moist static energy of days exceeding the x-th percentile of temperature in the historical simulation [i.e. $h_{\mathrm{L}}(p^{x}) \equiv h_{\mathrm{L}}^{x}$]. Note that, by the definition of moist static energy (1), the change in land moist static energy can also be written as:

$$\delta h_{\mathrm{L}}^{x} = c_p \delta T_{\mathrm{L}}^{x} + L_v \delta q_{\mathrm{L}}^{x}, \tag{4}$$

where $\delta T_{\mathrm{L}}^{x}$ and $\delta q_{\mathrm{L}}^{x}$ are the changes in land temperature and specific humidity, respectively, both averaged over all days exceeding the x-th percentile of temperature in the historical simulation.

The Δh term in (3) is estimated by considering the relationship between temperature, relative humidity and moist static energy on hot days. Over ocean, hotter days have larger moist static energies (Extended Data Fig. 1) because relative humidity is approximately uniform across percentiles of ocean temperature (Extended Data Fig. 2). But over land, where hotter days are drier[48] (Extended Data Fig. 2), the hottest 5% of days have a moist static energy equal to approximately the median land day, and become relatively less energetic as climate warms (Extended Data Fig. 1). This relative decrease with warming of the moist static energy of hot land days is quantified by Δh, which is well approximated as a function of changes in land relative humidity (Methods and Extended Data Fig. 3).

Combining (3) and (4) with the estimate of Δh, writing changes in specific humidity in terms of changes in saturation specific humidity and relative humidity and rearranging (Methods), the land temperature change for days exceeding the x-th percentile of temperature is estimated as a function of physical constants, properties of the climatological (historical) state and three components associated with changes in ocean temperature, ocean relative humidity and land relative humidity:

$$\delta T_{\mathrm{L}}^{x} = \left(\frac{1}{1 + \epsilon \delta r_{\mathrm{L}}^{x}} \right) \left(\gamma^{T_{\mathrm{O}}} \delta T_{\mathrm{O}} + \gamma^{r_{\mathrm{O}}} \delta r_{\mathrm{O}} - \eta \delta \overline{r_{\mathrm{L}}} \right), \tag{5}$$

where δT_{O} is the change in the p^x-th percentile of ocean temperature, r_{O} is the pseudo ocean relative humidity[41], r_{L}^{x} is the pseudo land relative humidity conditioned on T_{L}^{x} and $\overline{r_{\mathrm{L}}}$ is the mean pseudo land relative humidity (Methods). The parameters $\epsilon = L_v \alpha_{\mathrm{L}} q_{\mathrm{L,sat}}^{x} / (c_p + L_v \alpha_{\mathrm{L}} q_{\mathrm{L}}^{x})$ and $\eta = (\overline{q_{\mathrm{L,sat}}} / q_{\mathrm{L,sat}}^{x})(\epsilon / \alpha_{\mathrm{L}})$ are functions of physical constants, the climatological state and the Clausius-Clapeyron parameter α_{L}, which quantifies the fractional sensitivity of saturation specific humidity over land to a 1K temperature change. Note that $q_{\mathrm{L,sat}}^{x}$ is the land saturation specific humidity in the historical simulation conditioned on T_{L}^{x} and $\overline{q_{\mathrm{L,sat}}}$ is the mean land saturation specific humidity [saturation quantities are calculated following Bolton (1980)[49]]. The sensitivity parameters $\gamma^{T_{\mathrm{O}}} = (c_p + L_v \alpha_{\mathrm{O}} q_{\mathrm{O}}) / (c_p + L_v \alpha_{\mathrm{L}} q_{\mathrm{L}}^{x})$ and $\gamma^{r_{\mathrm{O}}} = L_v q_{\mathrm{O,sat}} / (c_p + L_v \alpha_{\mathrm{L}} q_{\mathrm{L}}^{x})$ quantify the sensitivities of land temperature to changes in ocean temperature and ocean relative humidity, respectively, holding other quantities in (5) fixed (Extended Data Fig. 4). [In the definitions of the sensitivity parameters $\gamma^{T_{\mathrm{O}}}$ and $\gamma^{r_{\mathrm{O}}}$ above, note that q_{O} and $q_{\mathrm{O,sat}}$ are the near-surface ocean specific humidity and saturation specific humidity in the historical simulation, respectively, and α_{O} is the Clausius-Clapeyron parameter for ocean.]

The theory (5) captures the key features of the multimodel-mean land temperature response across a wide range of percentiles, including the magnitude of the response (Fig. 2a) and amplified warming at high percentiles (Fig. 2b). Similar agreement between theory and simulations is found for the majority of individual models (Supplementary Figs. 1–5), and inter-model differences are very well explained by the theory (Extended Data Fig. 5). However a small number of models show disagreement between theory and simulations, perhaps due to moist static energies on hot land days being decoupled from neighbouring oceans in those specific models (in particular INM-CM4-8 and INM-CM5-0).

For constant land and ocean relative humidities, the theory simplifies to:

$$\delta T_{\mathrm{L,fix\ RH}}^{x} = \gamma^{T_{\mathrm{O}}} \delta T_{\mathrm{O}}. \tag{6}$$

This simple, fixed-relative humidity version of theory qualitatively captures the amplified warming of hot land days relative to the mean day (Fig. 2b), with the amplification driven by larger values of the sensitivity parameter $\gamma^{T_{\mathrm{O}}}$ for higher temperature percentiles (Extended Data Fig. 4a). The sensitivity parameter is larger for hot land days because those days are drier in terms of specific humidity (Extended Data Fig. 6) – this is the "drier get hotter" mechanism. The

land temperature response for fixed relative humidity (6) is strongly correlated across models with the simulated land temperature changes ($r = 0.93$ for the hottest 5% of land days). There is also a moderate correlation between simulated land temperature changes and the sensitivity parameter γ^{T_O} ($r = 0.45$ for the hottest 5% of land days), suggesting that approximately 20% of the variance across models in the warming of hot days over tropical land is explained by the climatological contrast in specific humidity between land and ocean regions.

Influence of relative humidity changes

I have shown that amplified warming of hot days over tropical land is a consequence of those days being dry. But changes in relative humidity affect the magnitude of the land temperature response across all percentiles (Fig. 2a) and, to a lesser extent, the degree to which warming of hot days is amplified (Fig. 2b). Small increases in ocean relative humidity with warming (Extended Data Fig. 2) – consistent with surface energy balance arguments[50, 46, 47] – marginally increase land warming by 0.11 K $\pm$ 0.06 K averaged across percentiles (Fig. 4). Increases in ocean relative humidity in a warming climate amplify increases in ocean specific humidity and moist static energy compared to a hypothetical scenario in which relative humidity stays constant. Changes in moist static energy over land and ocean are tightly coupled (Fig. 3), implying that the effect of increasing ocean relative humidity is to enhance moist static energy changes over land and therefore enhance land warming (Fig. 4). The component of the land warming associated with ocean relative humidity changes [see (5)] is very weakly correlated with the simulated land temperature responses ($r = 0.16$ for the hottest 5% of land days), indicating that changes in ocean relative humidity are not an important driver of the spread in land temperature changes across models.

Land relative humidity changes further increase the temperature response across percentiles (Fig. 4). Although the sensitivities of land temperature to 1% changes in land or ocean relative humidity are similar in magnitude (Extended Data Fig. 4b), the substantial decreases in land relative humidity with warming (Extended Data Fig. 2) contribute 0.38 K $\pm$ 0.22 K to the land temperature response averaged across percentiles (Fig. 4). The decrease in land relative humidity in a warming climate is a form of drying linked to the land-ocean warming contrast and changes in evapotranspiration[41, 9]. This drying inhibits increases in specific humidity over land. To compensate for the drying and satisfy the constraint of uniform changes in moist static energy across the tropics, land temperature increases are larger when land relative humidity decreases. The component of the theory associated with land relative humidity changes [see (5)] is strongly correlated with simulated land temperature changes ($r = 0.93$ for the hottest 5% of land days), highlighting that changes in relative humidity are key to understanding inter-model differences in projections of extreme temperatures over tropical land.

The contribution of land relative humidity changes to the land temperature

response has two components (Methods): The first quantifies the effect of a land relative humidity change on land temperature assuming $\Delta h = 0$, and the second quantifies the effect of a non-zero Δh [note that the Δh term is well approximated as a function of changes in land relative humidity (Methods)]. The first component (named δr_{L} comp.) enhances land warming (Fig. 4) because of the drying associated with land relative humidity decreases, as described in the paragraph above. The second component (named Δh comp.) counteracts the warming associated with the δr_{L} component (Fig. 4). In particular, the Δh component strongly tempers land warming at high percentiles. Note that $\Delta h < 0$ (Extended Data Fig. 3) meaning that hot land days become relatively less energetic as climate warms. In particular, the multimodel-mean moist static energy of the hottest 5% of land days is equal to the 54^{th} percentile of moist static energy in the historical simulation but only the 48^{th} percentile in the ssp245 simulation (Extended Data Fig. 1). This relative decrease in the moist static energy of hot land days with warming (i.e. $\Delta h < 0$), driven by decreases in land relative humidity, partly offsets the warming of extreme temperatures.

Numerous studies have emphasised the link between soil moisture, surface heat fluxes and extreme temperatures over land[14]. The theory developed here complements and expands this literature by linking warming of extreme temperatures to land relative humidity – a quantity tightly coupled to soil moisture[42] – via a simple equation (5). The theory also highlights the fundamental constraint on the combined response of temperature and specific humidity over tropical land – the moist static energy change – imposed by remote ocean warming, in contrast to the existing literature on extreme temperatures.

Synthesis and future directions

A new theory based on active convection and weak horizontal temperature gradients in the free troposphere quantitatively describes the simulated response of near-surface temperature over tropical land to climate change across a wide range of percentiles. The key prediction from the theory is that warming is amplified for hot land days because those days are dry: the "drier get hotter" mechanism. This mechanism provides a simple way in which to interpret changes in extreme temperatures in the tropics: To obey the constraint of approximately equal changes in moist static energy imposed by convection and weak temperature gradients, warming of hot land days is amplified to compensate for the limited increase in specific humidity due to those days being dry. The mechanism is predictive in the sense that it emerges from the climatological contrast in specific humidity between hot and less-hot days, and is not reliant on running a climate model. Amplified warming at high percentiles suggests that trends in the temperature of hot land days may be an early indicator of climate change in the tropics.

The magnitude of tropical land warming across percentiles is strongly enhanced by changes in relative humidity, with decreases in land relative humidity particularly important. Extending the theory to incorporate the influence of

land relative humidity changes as a function of the ocean warming and climatological state[41, 9] would be a natural next step, as would be the application of the theory to individual regions and to other climate perturbations (e.g. the El Niño/Southern Oscillation).

References

[1] Patz, J. A., Campbell-Lendrum, D., Holloway, T. & Foley, J. A. Impact of regional climate change on human health. *Nature* **438**, 310–317 (2005).

[2] Burke, M., Hsiang, S. M. & Miguel, E. Global non-linear effect of temperature on economic production. *Nature* **527**, 235–239 (2015).

[3] Seneviratne, S. I., Donat, M. G., Pitman, A. J., Knutti, R. & Wilby, R. L. Allowable CO_2 emissions based on regional and impact-related climate targets. *Nature* **529**, 477–483 (2016).

[4] Sutton, R. T., Dong, B. & Gregory, J. M. Land/sea warming ratio in response to climate change: IPCC AR4 model results and comparison with observations. *Geophys. Res. Lett.* **34** (2007). L02701.

[5] Lambert, F. H. & Chiang, J. C. H. Control of land-ocean temperature contrast by ocean heat uptake. *Geophys. Res. Lett.* **34** (2007). L13704.

[6] Joshi, M. M., Gregory, J. M., Webb, M. J., Sexton, D. M. H. & Johns, T. C. Mechanisms for the land/sea warming contrast exhibited by simulations of climate change. *Climate Dyn.* **30**, 455–465 (2008).

[7] Byrne, M. P. & O'Gorman, P. A. Land-ocean warming contrast over a wide range of climates: Convective quasi-equilibrium theory and idealized simulations. *J. Climate* **26**, 4000–4016 (2013).

[8] Byrne, M. P. & O'Gorman, P. A. Link between land-ocean warming contrast and surface relative humidities in simulations with coupled climate models. *Geophys. Res. Lett.* **40**, 5223–5227 (2013).

[9] Byrne, M. P. & O'Gorman, P. A. Trends in continental temperature and humidity directly linked to ocean warming. *Proc. Natl. Acad. Sci.* **115**, 4863–4868 (2018).

[10] Vogel, M. M. *et al.* Regional amplification of projected changes in extreme temperatures strongly controlled by soil moisture-temperature feedbacks. *Geophys. Res. Lett.* **44**, 1511–1519 (2017).

[11] Schär, C. *et al.* The role of increasing temperature variability in European summer heatwaves. *Nature* **427**, 332–336 (2004).

[12] Diffenbaugh, N. S. & Ashfaq, M. Intensification of hot extremes in the United States. *Geophys. Res. Lett.* **37** (2010).

[13] Mueller, B. & Seneviratne, S. I. Hot days induced by precipitation deficits at the global scale. *Proc. Natl. Acad. Sci.* **109**, 12398–12403 (2012).

[14] Seneviratne, S. I. *et al.* Impact of soil moisture-climate feedbacks on CMIP5 projections: First results from the GLACE-CMIP5 experiment. *Geophys. Res. Lett.* **40**, 5212–5217 (2013).

[15] Miralles, D. G., Teuling, A. J., Van Heerwaarden, C. C. & De Arellano, J. V.-G. Mega-heatwave temperatures due to combined soil desiccation and atmospheric heat accumulation. *Nat. Geosci.* **7**, 345–349 (2014).

[16] Lorenz, R. *et al.* Influence of land-atmosphere feedbacks on temperature and precipitation extremes in the GLACE-CMIP5 ensemble. *J. Geophys. Res.: Atmos.* **121**, 607–623 (2016).

[17] Screen, J. A. Arctic amplification decreases temperature variance in northern mid-to high-latitudes. *Nature Climate Change* **4**, 577–582 (2014).

[18] Schneider, T., Bischoff, T. & Płotka, H. Physics of changes in synoptic midlatitude temperature variability. *J. Climate* **28**, 2312–2331 (2015).

[19] Tamarin-Brodsky, T., Hodges, K., Hoskins, B. J. & Shepherd, T. G. Changes in Northern Hemisphere temperature variability shaped by regional warming patterns. *Nat. Geosci.* **13**, 414–421 (2020).

[20] Wehrli, K., Guillod, B. P., Hauser, M., Leclair, M. & Seneviratne, S. I. Identifying key driving processes of major recent heat waves. *J. Geophys. Res.: Atmos.* **124**, 11746–11765 (2019).

[21] Vargas Zeppetello, L. R. & Battisti, D. S. Projected increases in monthly midlatitude summertime temperature variance over land are driven by local thermodynamics. *Geophys. Res. Lett.* **47** (2020).

[22] McKinnon, K. A., Rhines, A., Tingley, M. P. & Huybers, P. The changing shape of Northern Hemisphere summer temperature distributions. *J. Geophys. Res.: Atmos.* **121**, 8849–8868 (2016).

[23] Linz, M., Chen, G. & Hu, Z. Large-scale atmospheric control on non-Gaussian tails of midlatitude temperature distributions. *Geophys. Res. Lett.* **45**, 9141–9149 (2018).

[24] Holmes, C. R., Woollings, T., Hawkins, E. & De Vries, H. Robust future changes in temperature variability under greenhouse gas forcing and the relationship with thermal advection. *J. Climate* **29**, 2221–2236 (2016).

[25] Pfahl, S. & Wernli, H. Quantifying the relevance of atmospheric blocking for co-located temperature extremes in the Northern Hemisphere on (sub-) daily time scales. *Geophys. Res. Lett.* **39** (2012).

[26] Liu, Q. On the definition and persistence of blocking. *Tellus A* **46**, 286–298 (1994).

[27] Seneviratne, S. I. *et al.* Investigating soil moisture-climate interactions in a changing climate: A review. *Earth-Sci. Rev.* **99**, 125–161 (2010).

[28] Donat, M. G. & Alexander, L. V. The shifting probability distribution of global daytime and night-time temperatures. *Geophys. Res. Lett.* **39**, L14707 (2012).

[29] O'Gorman, P. A. & Schneider, T. The physical basis for increases in precipitation extremes in simulations of 21st-century climate change. *Proc. Natl. Acad. Sci.* **106**, 14773–14777 (2009).

[30] O'Gorman, P. A. Contrasting responses of mean and extreme snowfall to climate change. *Nature* **512**, 416–418 (2014).

[31] Pfahl, S., O'Gorman, P. A. & Fischer, E. M. Understanding the regional pattern of projected future changes in extreme precipitation. *Nature Climate Change* **7**, 423–427 (2017).

[32] Perkins-Kirkpatrick, S. E. & Gibson, P. B. Changes in regional heatwave characteristics as a function of increasing global temperature. *Scientific Reports* **7**, 12256 (2017).

[33] Harrington, L. J. & Otto, F. E. L. Reconciling theory with the reality of African heatwaves. *Nature Climate Change* **10**, 796–798 (2020).

[34] Eyring, V. *et al.* Overview of the Coupled Model Intercomparison Project Phase 6 (CMIP6) experimental design and organization. *Geosci. Model Dev.* **9**, 1937–1958 (2016).

[35] O'Neill, B. C. *et al.* The Scenario Model Intercomparison Project (ScenarioMIP) for CMIP6. *Geosci. Model Dev.* **9**, 3461–3482 (2016).

[36] Zhang, Y. & Fueglistaler, S. How tropical convection couples high moist static energy over land and ocean. *Geophys. Res. Lett.* **47**, e2019GL086387 (2020).

[37] Duan, S. Q., Findell, K. L. & Wright, J. S. Three regimes of temperature distribution change over dry land, moist land and oceanic surfaces. *Geophys. Res. Lett.* e2020GL090997 (2020).

[38] Johnson, N. C. & Xie, S.-P. Changes in the sea surface temperature threshold for tropical convection. *Nature Geosci.* **3**, 842–845 (2010).

[39] Emanuel, K. A., Neelin, D. J. & Bretherton, C. S. On large-scale circulations in convecting atmospheres. *Quart. J. Roy. Meteor. Soc.* **120**, 1111–1143 (1994).

[40] Sobel, A. H., Nilsson, J. & Polvani, L. M. The weak temperature gradient approximation and balanced tropical moisture waves. *J. Atmos. Sci.* **58**, 3650–3665 (2001).

[41] Byrne, M. P. & O'Gorman, P. A. Understanding decreases in land relative humidity with global warming: conceptual model and GCM simulations. *J. Climate* **29**, 9045–9061 (2016).

[42] Berg, A. M. *et al.* Land-atmosphere feedbacks amplify aridity increase over land under global warming. *Nat. Climate Change* **6**, 869–874 (2016).

[43] Zhang, Y., Held, I. & Fueglistaler, S. Projections of tropical heat stress constrained by atmospheric dynamics. *Nat. Geosci.* **14**, 133–137 (2021).

[44] Sherwood, S. C. & Fu, Q. A drier future? *Science* **343**, 737–739 (2014).

[45] Chadwick, R., Good, P. & Willett, K. M. A simple moisture advection model of specific humidity change over land in response to SST warming. *J. Climate* **29**, 7613–7632 (2016).

[46] Held, I. M. & Soden, B. J. Water vapor feedback and global warming. *Annu. Rev. Energy Environ.* **25**, 441–475 (2000).

[47] Schneider, T., O'Gorman, P. A. & Levine, X. J. Water vapor and the dynamics of climate changes. *Rev. Geophys.* **48**, RG3001 (2010).

[48] Fischer, E. M. & Knutti, R. Robust projections of combined humidity and temperature extremes. *Nat. Climate Change* **3**, 126–130 (2013).

[49] Bolton, D. The computation of equivalent potential temperature. *Mon. Wea. Rev.* **108**, 1046–1053 (1980).

[50] Boer, G. J. Climate change and the regulation of the surface moisture and energy budgets. *Climate Dyn.* **8**, 225–239 (1993).

Methods

Simulations.

The following 18 climate models are analysed: ACCESS-CM2, ACCESS-ESM1-5, BCC-CSM2-MR, CanESM5, CESM2-WACCM, CNRM-CM6-1, CNRM-ESM2-1, GFDL-CM4, GFDL-ESM4, HadGEM3-GC31-LL, INM-CM4-8, INM-CM5-0, KACE-1-0-G, MIROC-ES2L, MPI-ESM1-2-LR, MRI-ESM2-0, NorESM2-LM and UKESM1-0-LL. Daily-mean near-surface temperature and specific humidity data from the historical (1980–2000) and ssp245 (2080–2100) simulations are used to investigate the response of tropical temperatures to climate change and to evaluate the theory.

Percentiles are computed at each latitude individually by aggregating daily-mean quantities over time and longitude. Before plotting, quantities are averaged from 20°S to 20°N with area weighting. Percentiles over land and ocean

are calculated separately. Similar results are obtained when the percentiles over land are computed at each gridpoint, by aggregating over time only, before being spatially averaged (Supplementary Fig. 6). Land is defined as all gridpoints where the percentage area occupied by land is greater than 50%; otherwise gridpoints are defined as ocean. Twenty six percentiles of temperature, specific humidity and moist static energy between the 0th and the 99th percentiles are computed; spline interpolation is used to estimate the percentiles between these computed values. The theory, derived below, is applied at each latitude individually before averaging the results from 20°S to 20°N.

Derivation of the theory for extreme temperatures over tropical land.

The key assumption underpinning the theory for the response of extreme temperatures over tropical land to climate change is that percentiles p of moist static energy h change equally over land (L) and ocean (O):

$$\delta h_{\mathrm{L}}(p) = \delta h_{\mathrm{O}}(p). \tag{7}$$

My focus is on hot days over land; the change in average moist static energy of days exceeding the x-th percentile of temperature between the historical and ssp245 simulations is given by:

$$\delta h_{\mathrm{L}}^{x} = c_p \delta T_{\mathrm{L}}^{x} + L_v \delta q_{\mathrm{L}}^{x}, \tag{8}$$

where $c_p = 1004.6$ J/kg/K is the specific heat capacity of air at constant pressure, $L_v = 2.5 \times 10^6$ J/kg is the latent heat of vapourisation, T_{L}^{x} is the near-surface land temperature (in kelvin) averaged over all days exceeding the x-th percentile of temperature and q_{L}^{x} is the average near-surface land specific humidity (in kg/kg) conditioned on T_{L}^{x}.

Defining p^x to be the moist static energy percentile over land corresponding to the average moist static energy of days exceeding the x-th percentile of temperature in the historical simulation [i.e. $h_{\mathrm{L}}(p^x) = h_{\mathrm{L}}^{x}$] and using the assumption of equal changes in moist static energy percentiles over land and ocean (7), the change in moist static energy of days exceeding the x-th percentile of temperature is expressed as:

$$\delta h_{\mathrm{L}}^{x} = \delta h_{\mathrm{O}}(p^x) + \Delta h, \tag{9}$$

where $\Delta h = h_{\mathrm{L}}^{\mathrm{ssp245}}(p^x + \delta p^x) - h_{\mathrm{L}}^{\mathrm{ssp245}}(p^x)$ quantifies the effect of a change in the percentile of land moist static energy to which hot land days correspond

(δp^x) on the moist static energy of those hot days. Note that $h_{\mathrm{L}}^{\mathrm{ssp245}}$ is the moist static energy in the ssp245 simulation, and that the presence of Δh in (9) is consistent with the assumption of equal changes in percentiles of moist static energy over land and ocean. As climate warms, hot land days become relatively less energetic ($\delta p^x < 0$; Extended Data Figs. 1 and 3a) implying that $\Delta h < 0$ (Extended Data Fig. 3b). The relative decrease in moist static energy of hot land days with warming (compared to a hypothetical scenario where $\delta p^x = 0$ and $\Delta h = 0$) limits the absolute increase in moist static energy, and has an important tempering influence on the response of extreme temperatures over tropical land to climate change.

Through (9), changes in the moist static energy of hot land days are related to changes in ocean moist static energy. Specifically, it is the change in the p^x-th percentile of ocean moist static energy that is relevant for hot land days. Over ocean, higher temperatures are associated with higher moist static energies (Extended Data Fig. 1) implying that the change in the p^x-th percentile of ocean moist static energy can be written to good approximation as a function of the individual changes in the p^x-th percentiles of temperature and specific humidity (Supplementary Fig. 7):

$$\delta h_{\mathrm{O}}(p^x) \approx c_p \delta T_{\mathrm{O}}(p^x) + L_v \delta q_{\mathrm{O}}(p^x). \tag{10}$$

Using (8) and (10), equation (9) can be written as:

$$c_p \delta T_{\mathrm{L}}^x + L_v \delta q_{\mathrm{L}}^x = c_p \delta T_{\mathrm{O}}(p^x) + L_v \delta q_{\mathrm{O}}(p^x) + \Delta h. \tag{11}$$

Defining pseudo relative humidities[41] over land [$r_{\mathrm{L}}^x = q_{\mathrm{L}}^x / q_{\mathrm{L,sat}}^x$] and ocean [$r_{\mathrm{O}} = q_{\mathrm{O}}(p^x)/q_{\mathrm{O,sat}}(p^x)$], where $q_{\mathrm{L,sat}}^x$ and $q_{\mathrm{O,sat}}(p^x)$ are the saturation specific humidities calculated using T_{L}^x and $T_{\mathrm{O}}(p^x)$, respectively, changes in specific humidity over land and ocean are written in terms of changes in temperature and pseudo relative humidity:

$$\delta q_{\mathrm{L}}^x = q_{\mathrm{L,sat}}^x \delta r_{\mathrm{L}}^x + \alpha_{\mathrm{L}} q_{\mathrm{L}}^x \delta T_{\mathrm{L}}^x + \alpha_{\mathrm{L}} q_{\mathrm{L,sat}}^x \delta r_{\mathrm{L}}^x \delta T_{\mathrm{L}}^x \text{ and} \tag{12}$$

$$\delta q_{\mathrm{O}} \approx q_{\mathrm{O,sat}} \delta r_{\mathrm{O}} + \alpha_{\mathrm{O}} q_{\mathrm{O}} \delta T_{\mathrm{O}}, \tag{13}$$

where $\alpha_{\mathrm{L}} = (\delta q_{\mathrm{L,sat}}^x / q_{\mathrm{L,sat}}^x)/\delta T_{\mathrm{L}}^x$ and $\alpha_{\mathrm{O}} = (\delta q_{\mathrm{O,sat}}/q_{\mathrm{O,sat}})/\delta T_{\mathrm{O}}$ are the Clausius-Clapeyron parameters defining the fractional sensitivities of land and ocean saturation specific humidities, respectively, to a 1K temperature change. For the change in ocean specific humidity (13), the nonlinear term associated with temperature and relative humidity changes has been omitted as it is negligible, but this term is substantial over land and is retained (12). Inserting expressions (12) and (13) into (11), dividing both sides by $c_p + L_v \alpha_{\mathrm{L}} q_{\mathrm{L}}^x$ and rearranging, I obtain the following expression for the land temperature response:

$$\delta T_{\mathrm{L}}^{x} = \left(\frac{1}{1+\epsilon\delta r_{\mathrm{L}}^{x}}\right)\left(\gamma^{T_{\mathrm{O}}}\delta T_{\mathrm{O}} + \gamma^{r_{\mathrm{O}}}\delta r_{\mathrm{O}} - [\epsilon/\alpha_{\mathrm{L}}]\delta r_{\mathrm{L}}^{x} + \Delta h\right), \tag{14}$$

where $\epsilon = L_v\alpha_{\mathrm{L}}q_{\mathrm{L,sat}}^{x}/(c_p + L_v\alpha_{\mathrm{L}}q_{\mathrm{L}}^{x})$. The parameters

$$\gamma^{T_{\mathrm{O}}} = \frac{c_p + L_v\alpha_{\mathrm{O}}q_{\mathrm{O}}}{c_p + L_v\alpha_{\mathrm{L}}q_{\mathrm{L}}^{x}} \text{ and} \tag{15}$$

$$\gamma^{r_{\mathrm{O}}} = \frac{L_v q_{\mathrm{O,sat}}}{c_p + L_v\alpha_{\mathrm{L}}q_{\mathrm{L}}^{x}} \tag{16}$$

quantify the sensitivities of land temperature to a unit change in ocean temperature or ocean relative humidity, respectively, assuming constant land relative humidity and $\Delta h = 0$ (Extended Data Fig. 4).

The Δh term in (14) is estimated as a function of the land temperature in the historical simulation and changes in land relative humidity. First, I approximate $\Delta h = h_{\mathrm{L}}^{\mathrm{ssp245}}(p^x + \delta p^x) - h_{\mathrm{L}}^{\mathrm{ssp245}}(p^x)$ as a Taylor series about $p = p^x$:

$$\Delta h = [h_{\mathrm{L}}(p^x + \delta p^x) - h_{\mathrm{L}}(p^x)] + [\delta h_{\mathrm{L}}(p^x + \delta p^x) - \delta h_{\mathrm{L}}(p^x)] \tag{17}$$

$$\approx \delta p^x \left(\left.\frac{\partial h_{\mathrm{L}}}{\partial p}\right|_{p=p^x} + \left.\frac{\partial}{\partial p}\delta h_{\mathrm{L}}\right|_{p=p^x}\right). \tag{18}$$

To estimate δp^x, I linearise the land moist static energy distribution in the historical simulation $h_{\mathrm{L}}(p)$ about its mean value:

$$h_{\mathrm{L}}(p) \approx \beta_1(p - \overline{p}) + \overline{h_{\mathrm{L}}}, \tag{19}$$

where $\overline{h_{\mathrm{L}}}$ is the mean moist static energy over land in the historical simulation, $\overline{p}$ is the moist static energy percentile corresponding to that mean value and $\beta_1 = \partial h_{\mathrm{L}}/\partial p|_{p=\overline{p}}$ is the slope of the tangent to the historical moist static energy distribution over land at $p = \overline{p}$ (Supplementary Fig. 8). The average moist static energy of days exceeding the x-th percentile of land temperature in the historical simulation is given by:

$$h_{\mathrm{L}}^{x} = c_p T_{\mathrm{L}}^{x} + L_v q_{\mathrm{L}}^{x}. \tag{20}$$

Combining (19) and (20), dropping the approximation symbol associated with (19) and noting that $h_{\mathrm{L}}(p^x) = h_{\mathrm{L}}^{x}$ by the definition of p^x, I find:

$$\beta_1(p^x - \overline{p}) + \overline{h_{\mathrm{L}}} = c_p T_{\mathrm{L}}^{x} + L_v q_{\mathrm{L}}^{x}. \tag{21}$$

Writing $T_{\mathrm{L}}^x = \overline{T_{\mathrm{L}}} + T_{\mathrm{L}}'$, $r_{\mathrm{L}}^x = \overline{r_{\mathrm{L}}} + r_{\mathrm{L}}'$ and $q_{\mathrm{L,sat}}^x = \overline{q_{\mathrm{L,sat}}} + q_{\mathrm{L,sat}}'$ [where $\overline{()}$ denotes a mean quantity and $()'$ denotes a departure from that mean], substituting into (21) and rearranging, I derive an expression for p^x:

$$p^x = \frac{1}{\beta_1}\left[c_p T_{\mathrm{L}}' + L_v(\overline{r_{\mathrm{L}}} q_{\mathrm{L,sat}}' + r_{\mathrm{L}}' \overline{q_{\mathrm{L,sat}}} + r_{\mathrm{L}}' q_{\mathrm{L,sat}}')\right] + \overline{p}. \tag{22}$$

Changes in the moist static energy percentile corresponding to the average moist static energy of days exceeding the x-th percentile of temperature (i.e. δp^x) are well approximated by truncating a linearised form of (22) to two terms (Extended Data Fig. 3a):

$$\delta p^x \approx \frac{L_v}{\beta_1}(\delta r_{\mathrm{L}}^x q_{\mathrm{L,sat}}^x - \delta\overline{r_{\mathrm{L}}}\,\overline{q_{\mathrm{L,sat}}}). \tag{23}$$

Inserting this estimate for δp^x into (18), defining $\beta_2 = \partial h_{\mathrm{L}}/\partial p|_{p=p^x}$ to be the slope of the tangent to $h_{\mathrm{L}}(p)$ at $p = p^x$, neglecting changes in β_2 with warming and further assuming $\beta_1 \approx \beta_2$ (Supplementary Fig. 8), Δh is found to be well approximated by (Extended Data Fig. 3b):

$$\Delta h \approx L_v(\delta r_{\mathrm{L}}^x q_{\mathrm{L,sat}}^x - \delta\overline{r_{\mathrm{L}}}\,\overline{q_{\mathrm{L,sat}}}). \tag{24}$$

Substituting (24) into (14) and rearranging, I derive an expression for the temperature response of days exceeding the x-th percentile of land temperature as a function of physical constants, climatological quantities and four components associated with Δh and changes in ocean temperature, ocean relative humidity and land relative humidity:

$$\delta T_{\mathrm{L}}^x = \left(\frac{1}{1+\epsilon\delta r_{\mathrm{L}}^x}\right)\left(\overbrace{\gamma^{T_{\mathrm{O}}}\delta T_{\mathrm{O}}}^{\delta T_{\mathrm{O}}\text{ comp.}} + \underbrace{\gamma^{r_{\mathrm{O}}}\delta r_{\mathrm{O}}}_{\delta r_{\mathrm{O}}\text{ comp.}} + \overbrace{[\epsilon/\alpha_{\mathrm{L}}][\delta r_{\mathrm{L}}^x - \delta\overline{r_{\mathrm{L}}}\,\overline{q_{\mathrm{L,sat}}}/q_{\mathrm{L,sat}}^x]}^{\Delta h\text{ comp.}}\right) \underbrace{-\left(\frac{1}{1+\epsilon\delta r_{\mathrm{L}}^x}\right)[\epsilon/\alpha_{\mathrm{L}}]\delta r_{\mathrm{L}}^x}_{\delta r_{\mathrm{L}}\text{ comp.}}. \tag{25}$$

The four components of the land temperature response are shown in Figure 4 along with their sum (δT_{O} comp. + δr_{O} comp. + Δh comp. + δr_{L} comp.), which is approximately equal to the full theory (25). [The small difference in Figure 4 between the full theory (25) and the sum of components arises from prescribing the pre-factor multiplying the δT_{O}, δr_{O} and Δh components to be equal to 1 for simplicity when summing the components.] The Δh and δr_{L} components

are both functions of changes in land relative humidity and can be combined into a *total* land relative humidity component:

$$\delta r_{\mathrm{L}}^{\mathrm{total}}\,\mathrm{comp.} = \Delta h\,\mathrm{comp.} + \delta r_{\mathrm{L}}\,\mathrm{comp.} = -\left(\frac{1}{1+\epsilon\delta r_{\mathrm{L}}^{x}}\right)\eta\delta\overline{r_{\mathrm{L}}}, \tag{26}$$

where $\eta = (\epsilon/\alpha_{\mathrm{L}})(\overline{q_{\mathrm{L,sat}}}/q_{\mathrm{L,sat}}^{x})$. Using (26), I arrive at the final form of the theory [see (5) in the main text]. Finally, based on (26) and taking $\delta r_{\mathrm{L}}^{x} = \delta\overline{r_{\mathrm{L}}}$ for simplicity, I define the sensitivity parameter

$$\gamma^{r_{\mathrm{L}}} = -\frac{\eta}{100+\epsilon} \tag{27}$$

which quantifies the sensitivity of land temperature to a 1% change in land relative humidity (Extended Data Fig. 4b).

Acknowledgements The author thanks Emily Newsom, Paul O'Gorman, Laure Zanna and Yi Zhang for helpful discussions. All analyses were performed using Pangeo, a community platform for Big Data geoscience (https://pangeo.io). MPB acknowledges support from the European Union's Horizon 2020 research and innovation programme under the Marie Sklodowska-Curie grant agreement no. 794063.

Competing Interests The author declares no competing interests.

Corresponding Author Correspondence and requests for materials should be addressed to the author (email: mpb20@st-andrews.ac.uk).

Author Contributions M.P.B. derived the theory, performed the analyses and wrote the manuscript.

Data Availability The CMIP6 model data are provided by the World Climate Research Programme's Working Group on Coupled Modelling and can be accessed at https://esgf-node.llnl.gov/search/cmip6/.

Code Availability The code used in this paper is available from the corresponding author on request.

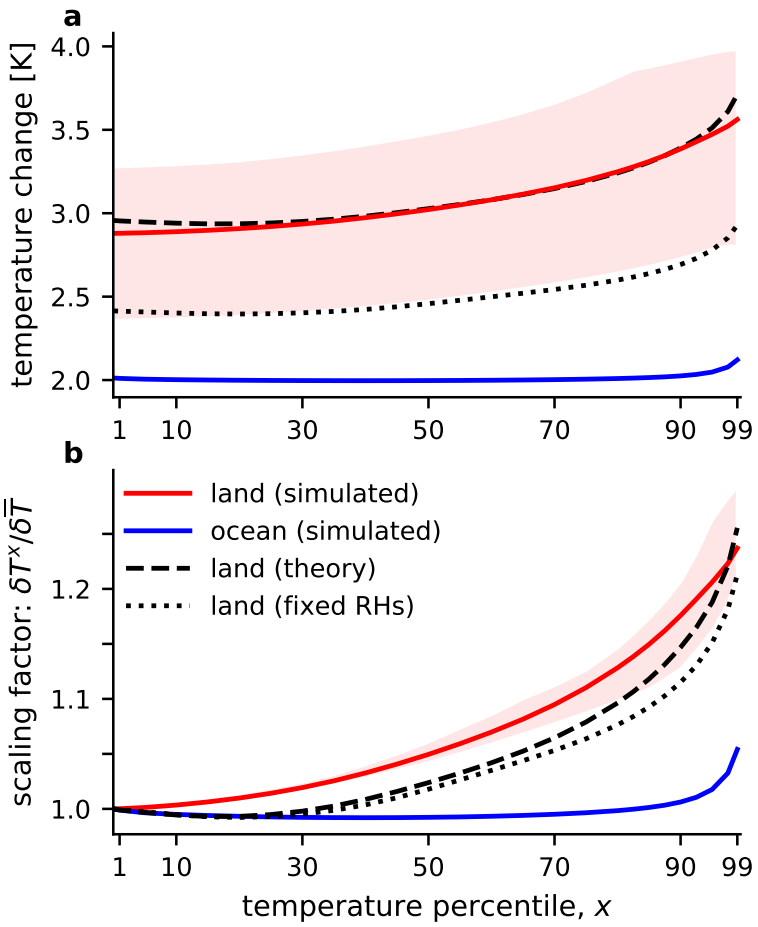

Figure 2: **Climate model projections and theoretical estimates of tropical land temperature responses across percentiles.** Multimodel-mean (a) near-surface temperature change and (b) scaling factor between the historical and Shared Socioeconomic Pathway 4.5 (ssp245) simulations for a range of daily-mean temperature percentiles (x) over land (red) and ocean (blue). Temperatures are averaged over days exceeding the x-th percentile of land or ocean temperature. The scaling factor is defined as the temperature change at each percentile (δT^x) normalised by the mean temperature change ($\delta\overline{T}$). Theory estimates of the land temperature change and scaling factor are also shown [dashed lines, see (5)] along with estimates from a version of the theory that assumes fixed relative humidities (RHs) over land and ocean [dotted lines, see (6)]. Shading indicates the model scatter for the land temperature change and scaling factor, with 50% of models lying within the shaded region. In this and subsequent figures, all quantities are spatially averaged from 20°S to 20°N.

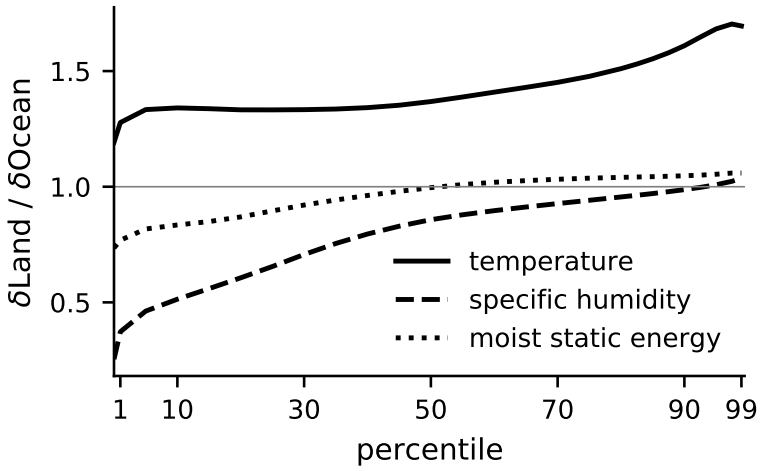

Figure 3: **Ratios of land-to-ocean changes in tropical temperature, specific humidity and moist static energy.** Land-to-ocean ratios of multimodel-mean changes in percentiles of near-surface temperature (solid black), specific humidity (dashed black) and moist static energy (dotted black) between the historical and Shared Socioeconomic Pathway 4.5 (ssp245) simulations.

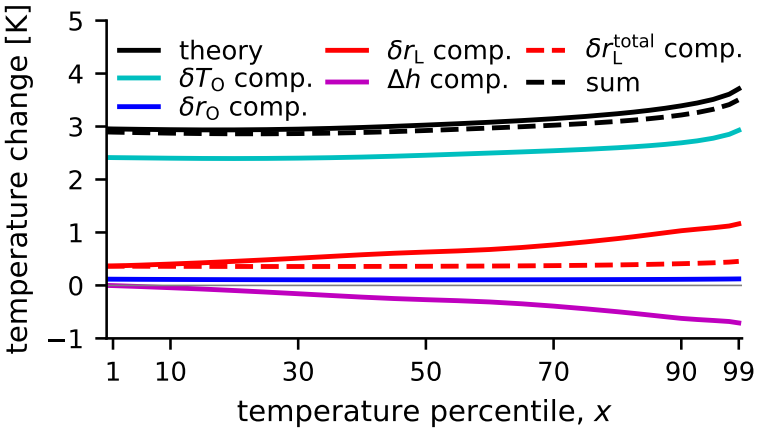

Figure 4: **Components of the land temperature response.** Multimodel-mean theory estimate of the land temperature change [solid black, see (5)] and the four components of the theory associated with changes in ocean temperature (δT_O; cyan), ocean relative humidity (δr_O; blue), land relative humidity (δr_L; solid red) and Δh (magenta). The sum of the four components (dashed black) is approximately equal to the full theory. The combined effect of changes in land relative humidity and Δh, the δr_L^{total} component, is indicated by the dashed red line (Methods).